Development Process of Shock Waves by Supersonic Spray

Kyoung-Su Im, and Ming-Chia Lai[1]

1. Department of Mechanical Engineering Wayne State University
Detroit, Michigan 48202 USA

Jin Wang [2]

2. Argonne National Laboratory, Argonne, Illinois 60439 USA

Abstract

In this study, we report a preliminary numerical simulation of shock wave generation by supersonic spray using the space-time CE-SE numerical scheme and the stochastic particle injection based on the Monte Carlo method. The 2-D test case simulates the injection of particles with poly-dispersed size distributions into a rectangular chamber filled with air at standard conditions. The initial injection velocity is 500 m/s, corresponding result in a 1.47 Mach number. For simplicity, the particle-to-particle interactions and the evaporation models are not applied in the calculation and only momentum coupling between the discrete-particle and continuous gas phases is considered using uncorrected drag correlations. A single spray injection case is used to simulate the spray-wall interactions; a dual spray injection is used to show spray-to-spray interactions. Favorable comparisons with the experimental results are demonstrated in terms of the physical characteristics of the shock wave generation and their interactions with spray and walls.

1. Introduction

Spray-shock interactions are a very complicated process. In general, two scenarios can occur, depending simplistically on if the particles are actively generating the shock waves or passively riding through them. The active case involves very high-velocity injection, which sometime occurs in diesel engine or water jet applications. The passive case can occur in a pulse detonation engine or a shock tube experiment. In either case, these interactions create a difficult challenge to determine their effects on the physical transport and possible chemical reaction processes. While the passive cases are studied more, perhaps arguably easier to set up experimentally, the active case is more complicated, because it usually involves dense spray and complicated multi-phase phenomena, which by themselves without the shock waves remain a technological challenge today.

In the diesel combustion, it is well known fact that the increase of the injection pressure effectively reduces the emissions in terms of NO_x and black smoke. In addition the combustion performance is greatly improved by forming the finer and more homogenous spray environment. Therefore, the challenging study of the high-pressure injection and its interaction with ambient gas in the combustion chamber has persistently been required. In the environment of the spray injection speed over sonic, the generation of the shock wave is naturally possible and thus, the interaction between spray particles and shock waves is of concern. One of the earlier research works was conducted by Nakahira et al. [1, 2]. During their study on the high-pressure spray into a pressure vessel, they found the weak shock wave generated when the fuel injection speed exceeds the ambient sonic velocity. In the subsequent work, they conducted to measure the droplet size and pressure amplitude to investigate the shock wave effects on the fuel spray. Following their findings, the shock

wave positively improve the spray atomization as decreasing the droplet size and the pressure amplitude of the shock wave was about 10% higher than that of ambient pressure. In addition, they suggested that verifying the mechanism of shock wave generation will clarify the mechanism of fuel jet break up and atomization.

Recently, Wang et al [6] demonstrated that high pressure fuel sprays in supersonic speed can generate the Mach cone in gaseous medium by directly imaging of x-radiography technique. This pioneering work in experimental technique of internal combustion engines makes it possible to obtain the qualitative data and allow the quantitative analysis of the shock wave parameters, simultaneously. Thus, they strongly believed that this methodology could be cleared out the dearth of experimental methods to validate computational modeling development.

Although high-speed particle streams or liquid jets have many scientific and engineering applications in medical surgery, manufacturing, cleaning, mining, and tunneling except diesel combustion engines, there are, so far, no research results of numerical simulations carried out on the subject due to difficulty in capturing shock wave structures and their interactions with discrete phase and wall boundary conditions. Therefore, there is a strong motivation to understand the generation mechanisms of shock wave by supersonic jet or spray. To this end, we attempt to tackle the active case in this paper to focus on the shock wave structure.

For simplicity, the deformation of the spray droplets is not taken into account; thus, the simulated processes more realistically resemble high-speed particle streams than spray. In addition, the slow down of acoustic speed in the two-phase mixture, in particular, for dense liquid sprays is also not taken into considerations in this study which is an another difficult challenge to numerical simulation. However, the present effort provides a steppingstone for future simulation of the spray-shock interactions, which could be present in future high-pressure diesel and pulse-detonation engines.

2. Theoretical model

2.1. Gas phase equations

The governing equations for the gas phase in numerical simulation are the two-dimensional Euler equations with spray source terms. The vector form of the governing equations are given by,

$$\frac{\partial \mathbf{U}}{\partial t}+\frac{\partial \mathbf{E}(\mathbf{U})}{\partial x}+\frac{\partial \mathbf{F}(\mathbf{U})}{\partial y}=\mathbf{S}(\mathbf{U}) \qquad (2.1)$$

where

$$\begin{aligned}\mathbf{U} &= (r, ru, rv, rE)^T \\ \mathbf{E}(\mathbf{U}) &= \left(ru, ru^2+p, ruv, (rE+p)u\right)^T \\ \mathbf{F}(\mathbf{U}) &= \left(rv, ruv, rv^2+p, (rE+p)v\right)^T \\ \mathbf{S}(\mathbf{U}) &= \left(\dot{m}, M_x, M_y, S_e\right)^T\end{aligned} \qquad (2.2)$$

In Eq. (2.2), r, u, v, p, and E, respectively, represent density, velocity, pressure, and specific total energy of the gas phase. The total energy E is defined as

$$E=e+\frac{1}{2}\left(u^2+v^2\right) \qquad (2.3)$$

where $e=p/(g-1)$ is the internal energy of the gas phase and $g=c_p/c_v$ is the ration of specific heats. The source terms appearing on the right-hand sides of the equations account for the particle effects. $\dot{m}$ is the additional change rate of gas phase mass due to the particle evaporation. M_x and M_y are the terms defining the x and y momentum exchange with the particles per unit volume. The energy source term S_e represents the work done by the particles on the gas. In present study, since we inject the spray into the quiescent ambient air in rectangular chamber as the stand state, i.e., 1 atm and room temperature, the rate of mass (the source term in mass equation) and the heat transfer from the particles to air, the source term in energy equation, are not considered. As a result, we only have the source terms for momentum equations. The $\boldsymbol{M_i}$ defining the drag on the gas due to the particles is given by,

$$\mathbf{M}_i=-\sum_k D_k(\mathbf{U})(\mathbf{U}-\mathbf{u}_k)d(\mathbf{x}-\mathbf{x}_k) \quad \text{i}=1,2 \qquad (2.4)$$

where the summation represnets the total number of particles in the calculation cell and $\delta(x)$ is the Dirac delta function, $D_k(\mathbf{U})$ is the

drag function, which will be described in following section.

2.2. Particle equations

In a Lagrangian reference frame [7], each particle, individually labeled by subscript k, is considered to obey the droplet governing equations. First, the drop position is given by

$$\frac{d\mathbf{x}_k}{dt} = \mathbf{u}_k \tag{2.5}$$

Then, the instantaneous particle velocity at arbitrary time is determined by solving the momentum equation.

$$m_k \frac{d\mathbf{u}_k}{dt} = m_k \mathbf{g} + D_k(\mathbf{U})(\mathbf{U} - \mathbf{u}_k) \tag{2.6}$$

where $D_k(\mathbf{U})$ is the draf function and given by

$$D_k(\mathbf{U}) = \frac{1}{2} p r_k^2 \rho_g C_D |\mathbf{U} - \mathbf{u}_k| \tag{2.7}$$

In Eq. (2.7), the drag coefficient is determined by [8]

$$C_D = \frac{24}{\mathrm{Re}_k}\left[1.0 + 0.15\,\mathrm{Re}_k^{0.687}\right] \quad \mathrm{Re}_k < 10^3$$
$$= 0.44 \qquad\qquad\qquad\qquad \mathrm{Re}_k > 10^3 \tag{2.8}$$

where Re_k is the particle Reynolds number which is evaluated by using relative velocity between the surrounding gas and particle, i.e.,

$$\mathrm{Re}_k = \frac{2 r_k |\mathbf{U} - \mathbf{u}_k| \rho_g}{\mu} \tag{2.9}$$

The energy equation of particles can be written as

$$m_k C_k \frac{dT_{sk}}{dt} = 4\pi r_k^2 h_k (T_g - T_k) - \dot{m}_k L \tag{2.10}$$

where h_k, the convective heat transfer coefficient and $\dot{m}_k$, the rate of particle evaporation are respectively given by

$$h_k = \frac{k_g}{r_k B_{Tk}} Nu \ln(1 + B_{Tk}) \tag{2.11}$$

and

$$\dot{m}_k = 4\pi r_k \left(\frac{k}{C_p}\right)_g Nu \ln(1 + B_{Tk}) \tag{2.12}$$

where B_{Tk} is the heat transfer number defined as

$$B_{Tk} = \frac{C_{pg}(T_g - T_k)}{L(T_k)} \tag{2.13}$$

where L is the latent heat of particle vaporization corresponding the particle temperature. In Eq.(2.11) and (2.12), the Nusselt number, Nu, is calculated by the following emperical correlation.

$$Nu = 1 + 0.3\,\mathrm{Re}_k^{0.5}\,\mathrm{Pr}_g^{0.33} \tag{2.14}$$

Note that in the present study, we only considered the source terms for momentum exchange. Thus, the Eq. (2.5)-(2.9) is used to generate the shock wave for the gas phase in rectangular chamber.

3. Numerical method

The space-time Conservation Element Solution Element (CESE) method, originally proposed by Chang [9, 10] has been applied to solve the spray-shock interaction flow. The space-time CESE method is a high-resolution and genuinely multidimensional method for solving conservation laws. It has a solid foundation in physics and yet is simple in mathematics. Its nontraditional features are: (i) a unified treatment of space and time, (ii) the introduction of conservation element (CE) and solution element (SE) as the vehicles for enforcing space-time flux conservation, and (iii) a time marching strategy that has a space-time staggered stencil at its core and, as such, can capture shocks without using Riemann solvers. Note that conservation elements are non-overlapping space-time subdomain introduced such that (i) the computational domain can be filled by these subdomains; and (ii) flux conservation can be enforced over each of them and also over the union of any combination of them. On the other hand, solution elements are non-overlapping space-time subdomains introduced such that (i) the boundary of any CE is covered by a combination of SEs; and (ii) within a SE, any physical flux vector is approximated using a simple smooth function. The implementation of the CESE method of spray is reported in [11].

4. Results and discussion

Figure 1 shows the initial and geometrical description of the simulation. Initially, gas flow field is at the standard-state conditions, 1 atm pressure and room

temperature (298.14K) without any velocity. Then, the supersonic particles assumed by probability density function are injected into the rectangular chamber based on a Monte Carlo technique. The injection nozzle has 160μm in diameter and the injection velocity was 500 m/s for all calculation, which is equivalent to 1.47 of Mach number. Two injection angles, i.e., 0 and 6 degree, were selected. The total calculation domain is 6cm × 2cm with the grid number of 1200×200.

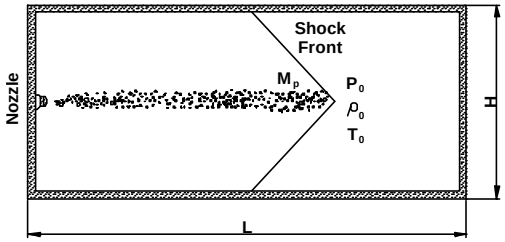

Figure 1 Schematic of the initial and geometrical settings for numerical simulation.

Figure 2 shows numerical Schlieren result of the generated shock structure with spray. The spray propagates from left to right along the axis of the injector. Here, the injection spray angle was 6° degree and the image was captured at 100μs. In [6] by using schlieren and X-ray imaging technique, they captured a weak shock wave at the top of the spray. In addition, their results provided that the generated shock wave was reflected from reflecting wall and propagated back into the spray. Similar to their results, the present result of the numerical schlieren image shows both the shock front and reflected shock clearly. Furthermore, a large number of internal shock waves are observed behind the main leading shock at the front, which is very similar to the results in [1~3].

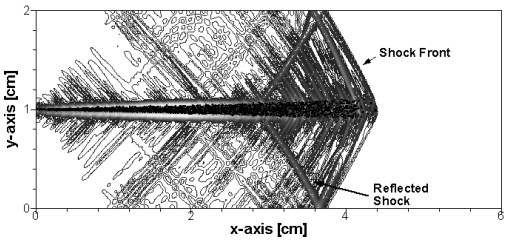

Figure 2 Numerical schlieren results.

Figure 3 shows time evolution of the pressure distributions superimposed with the spray. At the initial stage of development, i.e., up to 40μs, an oblique shock is clearly observed to form at the tip of the spray. When the generated shock wave reached the wall, it reflected and moved back into the flow with more increased shock strength. Referring to (e)~(j), the aerodynamics drag of the spray front has increased with increasing time. As a result, the leading shock became more round and weaker. In addition, several internal shock waves with more strength than that of leading shock are developed behind it.

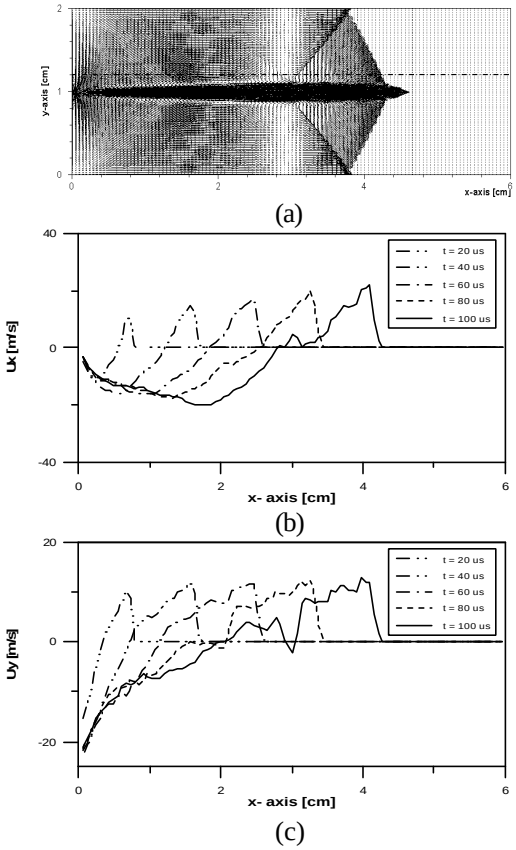

Figure 4 Velocity profiles of air field: (a) 2-dimensional distribution at time 100μs after injection with 6 degree injection angle, (b) x-velocity, and (c) y-velocity line profiles at different time extracted data along the dot line (y = 1.2cm) corresponding to the (a).

Figure 4 shows the velocity distributions of gas flow: (a) two-dimensional distribution, (b) x-velocity, and (c) y-velocity line profiles according to axial distance at y=1.2 cm with different time. In Figure 4(a), the formation of the leading shock and reflected shock is clearly observed. Since the high spray velocity along the center axis, the strong air

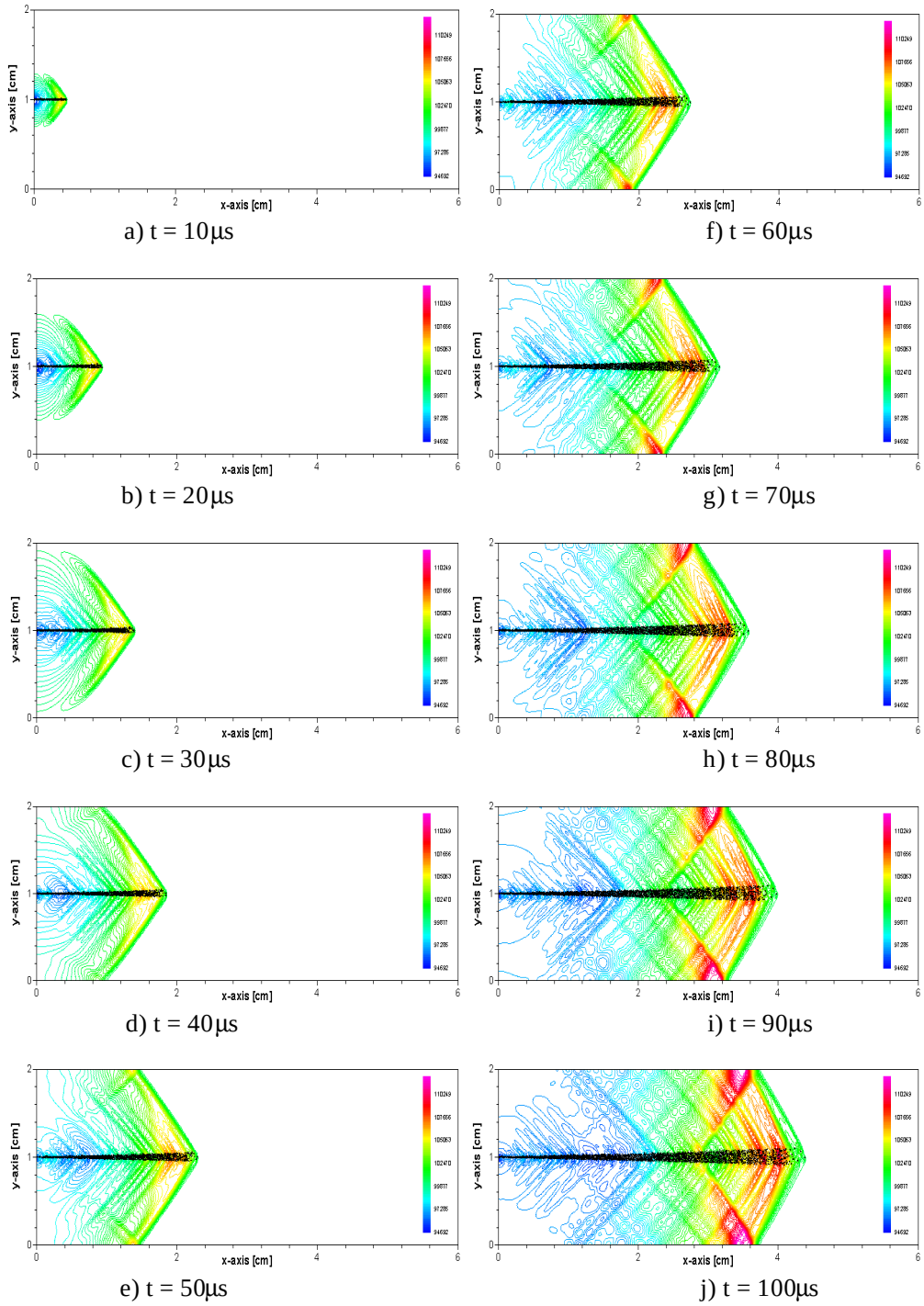

Figure 3 Time evolution of the shock wave generation by pressure distribution superimposed with supersonic spray

entrainment has developed at the location far from the leading shock, which can be more clearly shown in Figure 4(b) and (c) at time t=100 μs. In addition, the leading shock velocity is gradually increased according to time increasing, indicating that the shock wave is developing with increasing velocity strength.

Figure 5 is the plotting of the temperature distribution for two-dimensional, and line profiles extracted the value along the dot line corresponding to Figure 5(a) with different time. The hot temperature zone is formed between the leading shock and reflected shock. Refer to Figure 5(a). But an increment of temperature is yet small, i.e., only 5% increasing from initial temperature, indicating that the shock is not fully developed with the present calculation time. In Figure 5(b), the low temperature zone, less than initial temperature, is observed near the left wall. Since a large amount of the air entrainment exists in this area, this may be caused the reduction of the pressure energy, and thus, the temperature reduction. But, we would remark that the temperature of the shock front keep increasing with time.

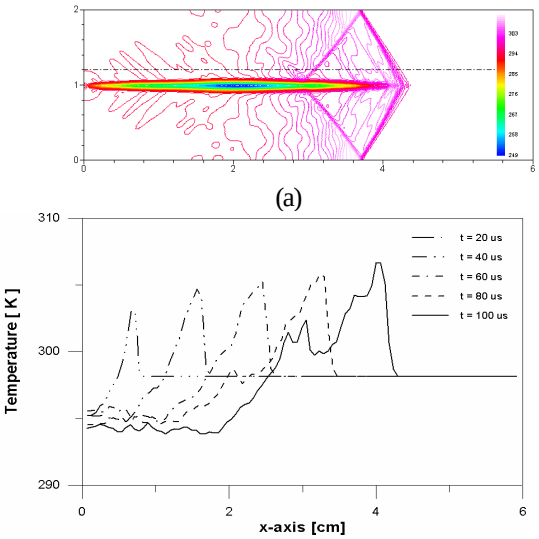

(a)

(b)

Figure 5 Temperature distributions of gas phase field: (a) 2-dimensional distribution at 100μs after spray injection without injection angle, (b) line profiles at different time extracted data along the dot line (y = 1.2cm) of the (a)

Figure 6 shows the air drag effects of spray particles for the ambient gas. At time t = 100 μs, the distribution of whole particles is plotted in Figure 6(a). Clearly, the small particles are easily influenced by air drag such that initial velocity is rapidly reduced according to axial distance. But the velocity reduction of big particles, less than 20 %, is much smaller than that of the small particles. Figure 6(b) illustrates more details for different particle size as a function of time. At 10 μm of particle diameter, the velocity reduction is significantly reduced for earlier time and it becomes small with time increasing. When the particle size is increased, the velocity gradient of air drag became constant, indicating that the big particles are not very sensitive from air drag since they have enough momentum to propagate.

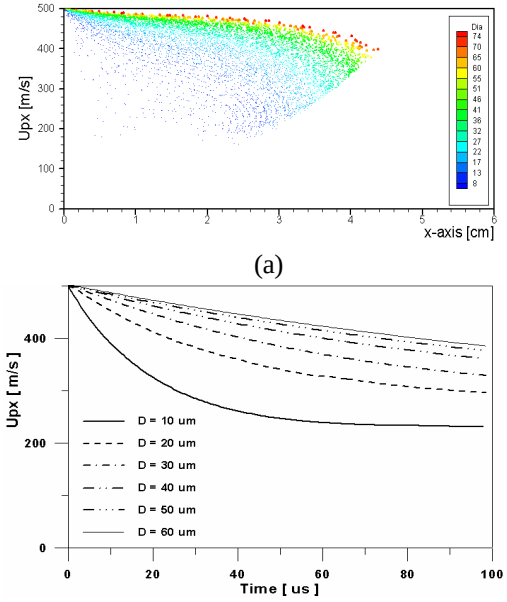

(a)

(b)

Figure 6 Aerodynamics drag effects of particles on the ambient air: (a) all distributed particles at time 100μs after injection without injection angle, (b) time histories for selected particle sizes as function of time.

Figure 7 shows pressure and schlieren contours for shock wave development by two-hole sprays. Both contours are taken at 100 μs after injection started. The calculation conditions are the same as the single spray except two sprays are injected with 30° of the spray angle and 2mm nozzle distance. The physical phenomenon is much more complicated than the single spray. First, the oblique shock waves attached on spray tips are

overlapped together along the center axis between two sprays and seem to make the pressure increasing on that region. Second, high pressure zones are constructed near upper and bottom walls by reflected shock waves. Third, when the reflected shock waves cross over the sprays, the part of shock waves transmits the spray and other parts are reflected to the spray. Finally, several reflected shock waves induced by internal shock waves from inside of sprays are interacting with other incoming shock waves from inside of sprays. Therefore, we believe that these complicated phenomenon will be positively affect to the spray atomization and thus, the combustion since reflected shock waves heat many times to the spray resulting in the small droplets and the several overlapped shock waves also definitely increase the mixture temperature. But further researches and precise analysis are needed to prove the present conclusions.

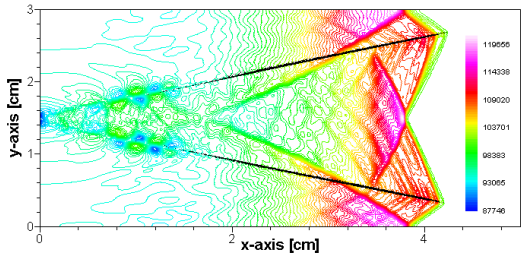

a)

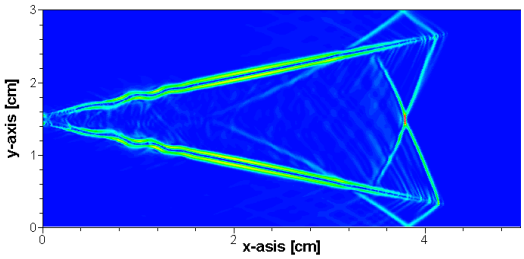

b)

Figure 7 Shock wave development by two-hole sprays with 30° of the spray angle and 2mm nozzle distance at conditions of 0° injection angle and 500 m/s of velocity: (a) pressure and (b) color schlieren distributions at time 100μs after injection.

5. Summary

A 2-D numerical simulations of the shock wave generation by supersonic spray have been conducted using the space-time CESE method and stochastic particle model with simple momentum coupling between the discrete and gas phases. The physical characteristics of shock wave generation and their interactions with each other, the discrete phases, and the walls are demonstrated. In addition, the following phenomena were observed:

i) the hot temperature zone between the leading shock and reflected shock,

ii) the re-circulation zone near the wall because of strong air entrainment, and

iii) the high sensitivity of air drag for the small particles and the constant gradient of air drag for the big particles.

6. Reference

[1]. Nakahira, T., Komori, M., Tsujimura, K., Suzuki, T., Obara, T., and Takayama, K., (1990) "Behavior of Shock Wave Generated around the Liquid Jet.," Dec., 1990 Shock Wave Symp., Tokyo (Japanese)

[2]. Nakahira,T., KomoriM., Nishida, M., and Tsujimura, K., 1992, "The Shock Wave Generation Around the Diesel Fuel Spray with High Pressure Injection" SAE paper 920460.

[3]. Nishida, K., Ochiai, H., Arai, M., and Hiroyasu, H. (1997) "Characterization of Diesel Fuel Spray by Ultrahigh-Pressure Injection," JSME Transc., 63(605), pp. 344-349.

[4]. Powell, C. F., Yue, Y., Poola, R., Wang, J., and Lai, M.-C., (2002) "A Quantitative Measurement of High-Pressure Dense Diesel Spray Core using Synchrotron X-Rays," *J. Engine*, SAE Transc. 110(3), pp. 422-429.

[5]. Powell, C. F., Yue, Y., Wang, J., and Lai, M.-C., (2001) "Quantitative X-Ray Characterization of a Diesel Spray Core," *ILASS AMERICAS '2001*, pp.71-75, May 20-23, Dearborn, Michigan.

[6]. Wang, J., et al., 2002, "Shock Waves Generated by High-Pressure Fuel Sprays Directly Imaged by X-

Radiography," SAE paper 2002-01-1892.

[7]. Amsden, A, A., O' Rourke, P. J., and Butler, T. D., (1989) "KIVA-II: A Computer Program for Chemically Reactive Flows with Sprays," Los Alamos Nat' l Lab. Report LA-11560-MS.

[8]. Clift, R., Grace, J. R., and Weber, M. E., (1978) "Bubbles, Drops, and Particles". Academic Press.

[9]. Chang, S.-C. (1995) "The Method of Space-Time Conservation Element and Solution Element- A New Approach for Solving the Navier-Stokes and Euler Equations," Journal of Computational Physics, Vol. 119, pp.295-324.

[10]. Chang, S.C., Wang, X.-Y. and Chow,1 C.-Y. (1999) "The method of Space-Time Conservation Element and Solution Element-A New High Resolution and Genuinely Multidimensional Paradigm for Solving Conservation Laws," J. Comput. Phys., 156 pp.89-136.

[11]. Im, K.-S., Yu, S.-T., Lai, M.-C., and Meredith, W. (2003) "Simulation of Spray Transfer Processes in Electrostatic Rotary Bell Sprayer," *J. Fluid Engineering*, accepted for publication.